Quantum theory of entangled-photon photoemission

Francesco Lissandrin,* Bahaa E. A. Saleh, Alexander V. Sergienko, and Malvin C. Teich†
Quantum Imaging Laboratory,‡ Departments of Electrical & Computer Engineering and Physics, Boston University, 8 Saint Mary's Street, Boston, Massachusetts 02215-2421, USA

(Received 28 August 2003; revised manuscript received 29 December 2003; published 27 April 2004)

A quantum theory of two-photon volume photoemission from metals and semiconductors is developed when the incident source of light comprises collinear down-converted entangled-photon pairs with entanglement time T_e. Despite the fact that the process involves the absorption of pairs of photons, the entangled-photon photocurrent varies linearly with the incident photon flux density. This is a consequence of the fact that the presence of one photon of an entangled-photon pair signals the presence of the other; it is in sharp contrast with the quadratic dependence of the classical two-photon photocurrent on incident photon flux density. Calculations are carried out for sodium metal (Na) and for K_2CsSb, a bialkali-antimonide semiconductor material often used as a cathode in photomultiplier tubes. The photocurrent is found to vary inversely with entanglement time although nonmonotonic behavior emerges over certain ranges of T_e. Entangled-photon photoemission may well be useful for enhancing the range of two-photon photoemission spectroscopy and might find particular use in the investigation of surface and image states of various materials.

DOI: 10.1103/PhysRevB.69.165317 PACS number(s): 79.60.Bm, 42.65.Lm, 03.65.−w

I. INTRODUCTION

The development of the laser in the early 1960s led to the blossoming of nonlinear optics.[1] Among the plethora of two-photon effects[1] that were first observed during that heady era was the two-photon photoelectric effect.[2,3] In the intervening years, two-photon photoemission, and two-photon photoemission spectroscopy, has been studied extensively and refined to the point that it has become a valuable tool for obtaining information about interface, surface, and image-potential states in various materials.[4–7]

The first theoretical treatment of the two-photon photoelectric effect was provided by Smith in 1962,[8] under the assumption that two-photon photoemission was a *surface* effect. Smith made use of the Sommerfeld model of a metal, and employed a second-order perturbation-theory calculation to calculate the photocurrent. However, it was subsequently determined that two-photon photoemission was a *volume* effect, and a suitable theory for this model was developed by Bloch in 1964.[9] Bloch's theory was based on the earlier first-order treatment of the ordinary (one-photon) photoeffect provided by Fan in 1945.[10] Both two-photon models predict a quadratic dependence of the two-photon photocurrent on incident photon flux density, as was, in fact, observed in experiments carried out in 1964 by Teich *et al.*[2,11,12] in Na metal and by Sonnenberg *et al.*[3] in Cs_3Sb semiconductor.

The emergence of optical coherence theory in the 1960s provided an impetus for examining how the statistical properties of light affected the magnitude of nonlinear interactions such as two-photon photoemission.[13] It was established early on, for example, that using excitation with thermal light, which has Bose-Einstein photon-counting statistics rather than the Poisson statistics of coherent light, results in a factor of 2 enhancement of the photocurrent.[13]

With the development of nonclassical sources of light in the 1980s (see, e.g., the review paper in Ref. 14), it is fitting to revisit this issue. In this paper, we provide a theoretical treatment of two-photon photoemission induced by a light source comprising entangled-photon pairs.

In particular, we consider the generation of such pairs via spontaneous parametric down-conversion in a second-order nonlinear optical crystal. This nonlinear optical process has a long and august history in quantum optics.[15–22] It leads to the production of a sequence of entangled photon pairs (so-called ''signal'' and ''idler'' photons with angular frequencies ω_1 and ω_2, respectively), each pair created by a single pump photon (angular frequency ω_p), such that energy and momentum are conserved. The process can be either of type I, in which the generated signal and idler photons have the same polarization, or of type II, in which they are orthogonally polarized. Moreover, the process can be collinear, in which the wave vectors of the signal and idler photons are parallel to that of the pump, or it can be noncollinear. The coherence properties of such sources have been studied extensively[23] and are now well understood. Partial entanglement has been determined to be a dual of partial coherence.[24] The focusing and imaging properties of entangled-photon pairs have also been established.[25,26]

This particular source of nonclassical light is of interest for two-photon photoemission by virtue of the fact that the photons are emitted in pairs;[27,28] the quantum state for each photon pair cannot be factored into a product of quantum states for the constituent photons.[15–17] Seminal early studies indicated that the two-photon absorption rate for entangled-photon pairs is linearly proportional to the photon flux density of the illuminating field.[29,30] This was a remarkable result in nonlinear optics since the two-photon absorption rate is almost always quadratic in the photon flux density. Another appealing feature of using entangled photons is the fact that the cross section for the rate of absorption of entangled photons can be enhanced relative to that of classical light for certain parameter values of the source, at least in simple atoms.[31,32]

Because of these unusual properties, several applications for such sources have been proposed, including entangled-photon virtual-state spectroscopy,[33,32] entangled-photon microscopy,[34] and entangled-photon lithography.[35]

Entangled-photon photoemission provides a natural choice for examining the interaction of entangled-photon light with matter since the nonlinear and detection processes are combined at a single locus and the behavior of the effect is well characterized for classical light. Furthermore, the effect results in the generation of charged electrons that are readily collected and measured by an electron multiplier, such as that in a photomultiplier tube.

In this paper we present a theory of entangled-photon volume photoemission for metals and semiconductors. Specific calculations are carried out for sodium metal (Na) and for the bialkali semiconductor K_2CsSb.[36] The latter material is of particular interest because of its wide use as a photocathode material in photomultiplier tubes; it is expected to provide a suitable choice for experimental studies of entangled-photon photoemission.

II. SEMICLASSICAL THEORY OF TWO-PHOTON VOLUME PHOTOEMISSION

A. Two-photon absorption cross section

The two-photon absorption cross section δ_r for an atomic transition from an initial state $|i\rangle$ to a final state $|f\rangle$, via a set of intermediate states $|j\rangle$, was calculated many years ago using semiclassical theory.[37–39] Assuming that the incident source of light is coherent and monochromatic (with angular frequency ω), and polarized along the x direction, and that the $\mathbf{A}\cdot\mathbf{p}$ term dominates the $\mathbf{A}^2$ term in the interaction Hamiltonian ($\mathbf{A}$ is the vector potential of the field and $\mathbf{p}$ is the electron momentum),[40,11] second-order perturbation theory yields

$$\delta_r = 2\pi^3 \frac{\hbar^2 r_0^2 c^2}{(\hbar\omega)^2}\,\delta\left(\frac{E_f - E_i - 2\hbar\omega}{\hbar}\right) \times\left[\left|\sum_j \frac{2\langle f|\hat{p}_x|j\rangle\langle j|\hat{p}_x|i\rangle}{m(E_j - E_i - \hbar\omega - i\hbar\kappa_j/2)}\right|^2\right]. \tag{1}$$

Here r_0 is the classical electron radius ($r_0 = e^2/mc^2$), e is the electronic charge, m is the mass of the electron, and c is the speed of light. The quantity δ represents the Dirac delta function; E_i, E_j, and E_f are the energies of the initial, intermediate, and final states, respectively; $\hbar$ is Planck's constant divided by 2π; κ_j is the intermediate-state linewidth; and $\hat{p}_x$ is the electron momentum operator.

Inasmuch as the semiclassical two-photon absorption rate R_r is given by[40]

$$R_r = \delta_r \phi^2, \tag{2}$$

the two-photon cross section δ_r is the proportionality constant between the transition rate R_r (sec^{-1}) and the square of the photon flux density ϕ^2 ($\mathrm{cm}^{-4}\,\mathrm{sec}^{-2}$), and as such has (cgs) units of cm^4 sec.

B. Two-photon photocurrent

At about the same time as the two-photon transition cross section was calculated, a semiclassical theory for the two-photon photoeffect in solids was developed using a closely related set of assumptions.[9,11,12] In this case the electron was initially assumed to be in the conduction band for a metal (valence band for a semiconductor) and the final state was taken to be the vacuum. This theory embodied a modification of the ordinary single-photon photoeffect theory developed by Fan,[10] in which perturbation-theory calculations were carried to second order. For simplicity of calculation, the theory dealt only with direct interband transitions and considered the electrons to be nearly free and to have Bloch-like wave functions. Inasmuch as both Na metal and K_2CsSb have nearly spherical Fermi surfaces[11,41] they more or less satisfy these assumptions. Moreover, it is known that indirect-band-gap materials are generally not good photoemitters.[41]

Using this approach, the classical two-photon photocurrent i_r is calculated by integrating over all possible initial momentum states k in the Brillouin zone[42] that can result in the escape of an electron from the surface of the material:[9,10]

$$i_r = e\frac{2Ad}{8\pi^3}\sum_f \frac{d}{dt}\int\int\int |a_{i,f}|^2 dk_x dk_y dk_z. \tag{3}$$

Here A is the illuminated area (spot size) and d is the electron escape depth so that Ad is the volume of the material involved in the photoemission process, and $|a_{i,f}|^2$ is the transition probability. The rate R_r of two-photon absorption from the initial state $|i\rangle$ to the final state $|f\rangle$ (the transition rate for the transition $i \to f$), in our notation, is given by the derivative of the transition probability:

$$\frac{d}{dt}|a_{i,f}(t)|^2 = \delta_r \phi^2. \tag{4}$$

Thus, the total two-photon photocurrent can be expressed as

$$i_r = (\beta\phi)^2 e\frac{2Ad}{8\pi^3}\sum_f \int\int\int \delta_r\, dk_x dk_y dk_z, \tag{5}$$

where an intensity-transmittance factor β is incorporated to accommodate reflection at the surface of the material.

For sodium metal it is safe to assume that the sphere in momentum space is uniformly filled to the Fermi energy. This is a reasonably good assumption for second-order perturbation-theory calculations, even when the temperature is greater than 0 K, although single-photon photoemission from the Fermi tail can come into play under these conditions[43] as discussed subsequently. It is also reasonable to assume that the Fermi surface is spherical for K_2CsSb since the material is nearly an intrinsic semiconductor whose Fermi energy is near the center of the band gap.[41] Moreover, photoeffects from multialkali materials are known to vary little with temperature.[44]

Integrating Eq. (5) over the initial k states, it can be shown that[9,11,12]

$$i_r = (\beta\phi)^2 e\frac{2Ad}{8\pi^3} 2\pi^3 m\frac{\hbar r_0^2 c^2}{(\hbar\omega)^2}\left[\left|\sum_j \frac{2\langle f|\hat{p}_x|j\rangle\langle j|\hat{p}_x|i\rangle}{m(E_j - E_i - \hbar\omega)}\right|^2\right] \times\frac{4}{3}\pi\frac{E_F}{2\hbar\omega}k_F\left[1 + \frac{eW}{E_F} - \frac{2\hbar\omega}{E_F}\right]^{3/2}. \tag{6}$$

The foregoing result is valid provided that the approximation that leads to Eq. (17a) of Ref. 9 [which is reproduced as Eq. (A16) in the Appendix, for convenience] is suitable, which is the case for many metals including Na. The quantity E_F represents the Fermi energy of the material, k_F is the wave number of an electron at the Fermi surface, and eW is the work function of the material. For semiconductors, the energy at the top of the valence band $E_{i\,\max}$ is used in the place of the Fermi energy E_F and $k_{i\,\max}$ replaces k_F. Alternatively, the photocurrent can be determined by numerically evaluating Eq. (16) of Ref. 9 [reproduced for convenience as Eq. (A15) in the Appendix], which is suitable for both Na and K_2CsSb. We choose this latter route.

Defining the transition matrix element (two-photon oscillator strength) as[11]

$$M \equiv \left| \sum_j \frac{2\langle f|\hat{p}_x|j\rangle\langle j|\hat{p}_x|i\rangle}{m(E_j - E_i - \hbar\omega)} \right|^2 \tag{7}$$

yields the final expression for the two-photon volume photocurrent induced by coherent light:[11,12]

$$i_r = \phi^2 \frac{\pi}{3} \frac{em\hbar r_0^2 c^2}{(\hbar\omega)^3} [M] \beta^2 A d E_F k_F \left[1 + \frac{eW}{E_F} - \frac{2\hbar\omega}{E_F} \right]^{3/2} = \eta_r e \Phi^2 / A, \tag{8}$$

where η_r is an efficiency. The dependence of the photocurrent on the strength of the excitation is governed by $\phi^2 A = \Phi^2/A \propto P^2/A$, where ϕ, Φ, and P represent the photon flux density (photons/cm^2 sec), photon flux (photons/sec), and optical power (W), respectively.

C. Two-photon oscillator strength

The two-photon oscillator strength was estimated to have the value $[M]_{\mathrm{Na}} = 8$ for Na under the assumptions that the **A·p** term in the Hamiltonian dominates and that intermediate states for the two-photon absorption process reside only in the final band.[11]

The two-photon oscillator strength for K_2CsSb, $[M]_{K_2CsSb}$, can be estimated by making use of the experimentally measured two-photon photocurrents for the two materials. Solving Eq. (8) for $[M]$ yields

$$[M] = i_r \frac{3}{\pi} \frac{(\hbar\omega)^3}{em\hbar r_0^2 c^2} \times \frac{1}{\phi^2 \beta^2 A d E_F k_F [1 + eW/E_F - 2\hbar\omega/E_F]^{3/2}}. \tag{9}$$

Forming a ratio of the values of $[M]$ for the two materials thus provides

$$\frac{[M]_{K_2CsSb}}{[M]_{\mathrm{Na}}} = \frac{i_r|_{K_2CsSb}}{i_r|_{\mathrm{Na}}} \frac{[(\hbar\omega)^3]_{K_2CsSb}}{[(\hbar\omega)^3]_{\mathrm{Na}}} \frac{[\phi^2\beta^2 A d E_F k_F (1 + eW/E_F - 2\hbar\omega/E_F)^{3/2}]_{\mathrm{Na}}}{[\phi^2\beta^2 A d E_{i\,\max} k_{i\,\max} (1 + eW/E_{i\,\max} - 2\hbar\omega/E_{i\,\max})^{3/2}]_{K_2CsSb}}, \tag{10a}$$

under the assumption that the approximation inherent in Eq. (A16) is suitable. Equation (10a) is readily rewritten in terms of the ratio of the double-quantum photoelectric yields[12] Λ for the two materials, since $\Lambda = i_r/P \propto i_r/\phi A$. The responsivity Λ has units of A/W and is itself proportional to ϕ. Equation (10a) thus becomes

$$\frac{[M]_{K_2CsSb}}{[M]_{\mathrm{Na}}} = \frac{\Lambda_{K_2CsSb}}{\Lambda_{\mathrm{Na}}} \frac{[\beta^2 d E_F k_F (1 + eW/E_F - 2\hbar\omega/E_F)^{3/2}]_{\mathrm{Na}}}{[\beta^2 d E_{i\,\max} k_{i\,\max} (1 + eW/E_{i\,\max} - 2\hbar\omega/E_{i\,\max})^{3/2}]_{K_2CsSb}}. \tag{10b}$$

The two-photon oscillator strength for K_2CsSb, $[M]_{K_2CsSb}$, may therefore be estimated by making use of the two-photon oscillator strength for Na determined previously,[11] along with the known parameters of the two materials and their measured double-quantum yields.

However, we choose to avoid the approximation inherent in Eq. (A16), which is almost certainly valid for Na but may not be for K_2CsSb, by instead numerically integrating Eq. (A15) over k, whereupon Eq. (10b) is replaced by

$$\frac{[M]_{K_2CsSb}}{[M]_{\mathrm{Na}}} = \frac{\Lambda_{K_2CsSb}}{\Lambda_{\mathrm{Na}}} \frac{[\beta^2 d \int_{k_{\min}}^{k_F} [k/\sqrt{k^2 + (2m/\hbar)2\omega} - k] dk]_{\mathrm{Na}}}{[\beta^2 d \int_{k_{\min}}^{k_F} [k/\sqrt{k^2 + (2m/\hbar)2\omega} - k]\, dk]_{K_2CsSb}}. \tag{10c}$$

D. Single-photon photoemission from the Fermi tail

The small magnitude of the two-photon photocurrent makes it important to carry out experimental measurements in such a way that single-photon photoemission is suppressed, lest it mask the two-photon photocurrent. The wavelength of the incident light must therefore be chosen such that its photon energy is smaller than the work function of the material (to avoid single-photon photoemission) but

greater than half the work function of the material (to ensure that two photons impart sufficient energy for electron escape):

$$\frac{eW}{2} < \hbar\omega < eW. \tag{11}$$

Even under these conditions, however, a single photon can give rise to photoemission via thermally excited electrons in the tail of the Fermi distribution. The probability of this process can be reduced by choosing the photon energy to be just greater than half the work function of the material and by reducing the temperature of the material to reduce the Fermi tail.[2,43]

III. QUANTUM THEORY OF ENTANGLED-PHOTON PHOTOEMISSION

When coherent light is used as the source of excitation, it is clear from the results provided in Sec. II that the two-photon absorption and photoemission rates are proportional to the square of the photon flux density. Although the magnitude of the rate depends on the statistical properties of the light, as pointed out in Sec. I, the proportionality of the rate to ϕ^2 remains intact for all sources of classical light. This is not necessarily true for nonclassical light.

We proceed to derive an expression for the two-photon photocurrent i_e when the source of excitation comprises entangled-photon pairs. In this case the entangled-photon photoemission rate turns out to be proportional to ϕ rather than to ϕ^2.[29–31]

A. Spontaneous optical parametric down-conversion

The center angular frequencies of the signal and idler wave packets are denoted ω_1^0 and ω_2^0, respectively. The entangled-photon pairs are characterized by an entanglement time T_e and an entanglement area A_e, representing the widths of the fourth-order temporal and spatial coherence functions, respectively.[23] The entanglement time is a measure of the mean time delay between the arrival of a photon and its entangled twin. It is governed principally by the length of the nonlinear crystal in which the pairs are generated inasmuch as photons of different wavelengths, directions of travel, and/or polarizations experience different mean delays as they pass through the nonlinear crystal, by virtue of dispersion in the medium and/or material thickness. A small entanglement time signifies that the photons arrive closely in time, a condition that is usually desirable. This is most readily achieved by using a thin nonlinear crystal.

Calculations will be explicitly carried out for collinear optical parametric down-conversion in a nonlinear optical crystal of length l, pumped by a monochromatic laser beam with wave number k_p.

B. Entangled-photon absorption cross section

We consider the entangled-photon cross section σ_e for a transition from an initial state $|i\rangle$ to a final state $|f\rangle$, via a set of intermediate states $|j\rangle$. This cross section was calculated by Fei *et al.*[31] in the context of a fully quantum mechanical treatment for transitions between discrete atomic levels, in second-order perturbation theory. Converting Fei *et al.*'s result from natural to cgs units and considering the special case of a monochromatic pump yields

$$\sigma_e = \frac{\pi}{4A_eT_e}(2\pi)^2\frac{r_0^2c^2}{\omega_1^0\omega_2^0}\delta\left(\frac{E_f-E_i-\hbar\omega_p}{\hbar}\right) \times\left|\sum_j\left\{\langle f|\hat{p}_{x,2}|j\rangle\langle j|\hat{p}_{x,1}|i\rangle\frac{1-e^{-iT_e(E_j-E_i-\hbar\omega_1^0)/\hbar-T_e\kappa_j/2}}{m(E_j-E_i-\hbar\omega_1^0-i\hbar\kappa_j/2)}+\langle f|\hat{p}_{x,1}|j\rangle\langle j|\hat{p}_{x,2}|i\rangle\frac{1-e^{-iT_e(E_j-E_i-\hbar\omega_2^0)/\hbar-T_e\kappa_j/2}}{m(E_j-E_i-\hbar\omega_2^0-i\hbar\kappa_j/2)}\right\}\right|^2, \tag{12}$$

where the κ_j are phenomenological intermediate-state linewidths, which in general depend on the photon flux density but can be considered constant for sufficiently weak light.[31]

The terms within the absolute square in Eq. (12) can interfere and, in general, lead to nonmonotonic behavior of σ_e with T_e, including the possibility of entanglement-induced two-photon transparency for certain values of T_e. Both the origin of this interference and its behavior for the $1S$-$2S$ two-photon transition in atomic hydrogen have been examined in detail by Fei *et al.*[31]

The entangled-photon absorption rate (photons/sec) for an electron transition is given by

$$R_e = \frac{d}{dt}|a_{i,f}(t)|^2 = \sigma_e\phi, \tag{13}$$

which indicates that the entangled-photon cross section σ_e has (cgs) units of cm^2. The linear dependence of R_e on the photon flux density ϕ accords with early predictions[29,30] and with recent quantum mechanical calculations.[31] As indicated above, this behavior is in sharp contrast with that for classical light, which exhibits a quadratic dependence on the photon flux density, in accordance with Eq. (2). Moreover, the harmonic terms in Eq. (12) clearly intertwine the entanglement characteristics of the source with the parameters of the medium in a generally nonfactorizable fashion.

C. Critical photon-flux density

The entangled-photon absorption rate $R_e = \sigma_e\phi$ must be supplemented by the absorption rate representing the accidental arrival of pairs $R_r = \delta_r\phi^2$ from the source of entangled light. The two photons that induce absorption in the former

case are colloquially referred to as ''twins,'' whereas those in the latter case are referred to as ''cousins.'' The overall two-photon absorption rate is then

$$R = R_e + R_r = \sigma_e \phi + \delta_r \phi^2, \tag{14}$$

where δ_r is given by Eq. (1) and σ_e is given by Eq. (12). For a single atom, therefore, two-photon absorption is dominated by entangled-photon pairs (twins) only for a sufficiently small photon-flux density. The critical photon-flux density ϕ_c at which the two processes are equal is given by

$$\phi_c = \sigma_e / \delta_r . \tag{15}$$

We will see subsequently that the overall entangled-photon photocurrent elicited from a bulk sample depends on the incident photon flux Φ rather than on the photon-flux density ϕ, whereas the two-photon photocurrent expressly depends on ϕ. Entangled-photon photoemission can therefore be enhanced relative to two-photon photoemission by reducing ϕ, which may be operationally achieved by defocusing the beam of light incident on the material.

A simple probabilistic model that considers the twin photons as particles has been set forth previously.[31] Although, by construction, this model cannot exhibit the interference inherent in Eq. (12), it nevertheless provides some indication of the expected magnitudes of the cross sections δ_r and σ_e. Within the confines of this model, the entangled two-photon cross section can be written as

$$\sigma_e = \frac{\delta_r}{2 A_e T_e}. \tag{16}$$

Combining Eqs. (15) and (16) yields a simple result for the critical photon-flux density,

$$\phi_c = \frac{1}{2 A_e T_e}; \tag{16a}$$

however, this phenomenological result must be viewed with caution. For the source of entangled photons at hand, the entanglement time and entanglement area are estimated to be $T_e = 10$ fsec and $A_e = 100\ \mu\text{m}^2$, respectively, so that $\phi_c = 1/2 A_e T_e = 5 \times 10^{19}$ photons/cm^2 sec.

D. Simple particlelike model

For a nondepleted pump, the entangled-photon photocurrent is given by

$$i_e = \beta^2 e N \sigma_e \phi A d = \beta^2 e N \sigma_e \Phi d = \eta_e e \Phi, \tag{17}$$

where β is the intensity transmittance through the surface of the material, e is the electronic charge, N is the atomic density (or in semiconductors the number of primitive cells per unit volume) of the medium (cm^{-3}), σ_e is the atomic entangled-photon cross section (cm^2), ϕ is the photon flux density (photons/cm^2 sec), A is the area illuminated (cm^2), Φ is the photon flux (photons/sec), and d is the depth of photoemission (cm). Using this phenomenological model, the entangled-photon photoemission efficiency of the material η_e (electrons/photon) is therefore given by

$$\eta_e = \beta^2 N \sigma_e d. \tag{18}$$

As promised earlier, the entangled-photon photocurrent i_e in Eq. (17) is linearly dependent on the photon flux Φ. In the context of the simple particlelike model, this dependence arises because the arrival of one photon of an entangled pair indicates with certainty that its twin is close behind (for coherent photons, the arrival of one photon indicates nothing about the arrival of another, which yields the Φ^2 dependence). Nevertheless, the dependence of the entangled-photon photocurrent i_e on the intensity transmittance β in Eq. (17) remains quadratic since the loss of either of the twins results in the loss of the pair. By virtue of its proportionality to Φ (photons/sec), i_e is independent of the area of illumination, provided that the beam is within the entanglement area, an important feature that is in sharp contrast with two-photon photoemission.

E. Entangled-photon photocurrent

We now calculate the entangled-photon photocurrent by proceeding along the same lines used in Sec. II, assuming volume photoemission, direct interband transitions, Bloch-like wave functions for the initial and final states, and spherical Fermi surfaces.

The entangled-photon photocurrent i_e is calculated by integrating over all possible initial momentum states k in the Brillouin zone,[42] as in Eq. (3), so that

$$i_e = \phi \beta^2 e \frac{2Ad}{8\pi^3} \sum_f \int\int\int \sigma_e \, dk_x dk_y dk_z , \tag{19}$$

which is analogous to Eq. (5) for two-photon photoemission. The dependencies in Eq. (19) are identical to those in the simple particle model, as provided in Eq. (17).

In metals and semiconductors, the discrete energy states are spaced sufficiently closely that they form bands. Using the usual parabolic energy-momentum relation

$$E_j = E_c + \frac{\hbar^2 k^2}{2m} \tag{20}$$

yields a density of intermediate states (per unit energy per unit volume) given by[45]

$$\rho(E_j) = \frac{(2m)^{3/2}}{2\pi^2 \hbar^3} (E_j - E_c)^{1/2}. \tag{21}$$

Assuming that the only intermediate states that contribute to the transition themselves lie in the final-states band, as discussed subsequently, E_j and E_c represent the energies of the intermediate states and the minimum energy for the final-states band, respectively, and m is the electron mass. The probability of finding an available state between energy E_j and $E_j + dE_j$ is therefore given by

$$p(E_j)dE_j = Ad\frac{(2m)^{3/2}}{2\pi^2\hbar^3}(E_j-E_c)^{1/2}dE_j \Big/ Ad\int_{E_{j\,\min}=E_c}^{E_{j\,\max}}\rho(E_j)dE_j = \frac{1}{N_j}\frac{(2m)^{3/2}}{2\pi^2\hbar^3}(E_j-E_c)^{1/2}dE_j, \tag{22}$$

where the total number of intermediate states per unit volume is

$$N_j = \int_{E_{j\,\min}=E_c}^{E_{j\,\max}}\rho(E_j)dE_j. \tag{23}$$

Following earlier treatments,[11,12] it is assumed that the intermediate states that contribute significantly to the photocurrent lie in the final-states band for both Na and K_2CsSb. The summation over the intermediate states j in Eq. (12) is therefore replaced by an integral over a continuum of intermediate states within the energy range $[E_{j\,\min},E_{j\,\max}]$. Finally, then, combining Eqs. (12), (19), and (22) yields

$$i_e = \phi\beta^2 e\frac{2Ad}{8\pi^3}(2\pi)^2\frac{r_0^2c^2}{\omega_1^0\omega_2^0}\frac{\pi}{4A_eT_e}\sum_f\int\int\int\delta\left(\frac{E_f-E_i-\hbar\omega_p}{\hbar}\right)\left|\int_{E_{j\,\min}}^{E_{j\,\max}}\left\{\langle f|\hat{p}_{x,2}|j\rangle\langle j|\hat{p}_{x,1}|i\rangle\right.\right.$$
$$\left.\left.\times\frac{1-e^{-iT_e(E_j-E_i-\hbar\omega_1^0)/\hbar-T_e\kappa_j/2}}{m(E_j-E_i-\hbar\omega_1^0-i\hbar\kappa_j/2)}+\langle f|\hat{p}_{x,1}|j\rangle\langle j|\hat{p}_{x,2}|i\rangle\frac{1-e^{-iT_e(E_j-E_i-\hbar\omega_2^0)/\hbar-T_e\kappa_j/2}}{m(E_j-E_i-\hbar\omega_2^0-i\hbar\kappa_j/2)}\right\}p(E_j)dE_j\right|^2 dk_xdk_ydk_z. \tag{24}$$

Intermediate states are assumed to comprise a continuous band and transitions involving them need not conserve crystal momentum.

As shown in the Appendix, Eq. (24) simplifies to [see Eqs. (A14), (A6), and (A13)]

$$i_e = \phi\beta^2 Ad\frac{em^4r_0^2c^2}{4\pi^3\hbar^5}\frac{\omega_p^2}{4\omega_1^0\omega_2^0}\mu\frac{1}{A_eT_e}\times\int_{k_{\min}}^{k_F}\frac{F(k,T_e)}{\sqrt{k^2+(2m/\hbar)\,\omega_p}-k}k\,dk, \tag{25}$$

with

$$F(k,T_e) = \left|\int_{E_{j\,\min}}^{E_{j\,\max}}\left\{\frac{1-e^{-i(T_e/\hbar)(E_j-\hbar^2k^2/2m-\hbar\omega_1^0)-T_e\kappa_j/2}}{E_j-\hbar^2k^2/2m-\hbar\omega_1^0-i\hbar\kappa_j/2}\right.\right.$$
$$\left.\left.+\frac{1-e^{-i(T_e/\hbar)(E_j-\hbar^2k^2/2m-\hbar\omega_2^0)-T_e\kappa_j/2}}{E_j-\hbar^2k^2/2m-\hbar\omega_2^0-i\hbar\kappa_j/2}\right\}\times\sqrt{E_j-E_c}\,dE_j\right|^2, \tag{26}$$

where $k=\sqrt{2mE_i/\hbar^2}$ and

$$\mu = \left[\left|\frac{4\langle f|\hat{p}_x|j\rangle\langle j|\hat{p}_x|i\rangle}{m\hbar\omega_p}\right|^2\right]_{\rm av}\Big/N_j^2. \tag{27}$$

It is of interest to observe that the complex exponential terms in Eq. (26), which are characteristic of the photon entanglement, depend on the entanglement time T_e. Thus, the entangled-photon photocurrent can exhibit nonmonotonic behavior as T_e is altered.

The magnitude of the entangled-photon photocurrent in Eq. (25) is clearly proportional to $\phi A=\Phi\propto P$, where ϕ, Φ, and P again represent the photon-flux density (photons/cm^2 sec), photon flux (photons/cm^2), and optical power P, respectively. As indicated previously, in contradistinction to the classical two-photon photocurrent, the entangled-photon photocurrent depends on the total power of the incident beam so that the degree of focusing of this beam is immaterial. Simple defocusing of the incident light then serves to decrease the contribution of cousins to the photocurrent but does not inhibit that of twins, provided, however, that the defocusing does not concomitantly change the entanglement area A_e.

IV. RESULTS

A. Entangled-photon photocurrent

Using Eqs. (25)–(27), we proceed to calculate the entangled-photon photocurrent i_e as a function of the entanglement time T_e, for Na metal and K_2CsSb. We effect this calculation in the context of the simplified energy-band diagrams illustrated in Fig. 1. Results for the sodium and bialkali-semiconductor photocurrents are presented in Figs. 2 and 3, respectively, for several values of the nondegeneracy ratio: $\omega_1^0/\omega_p=1/2$, 1/3, and 1/8 ($\omega_1^0+\omega_2^0=\omega_p$). The entangled-photon photocurrents are also compared with the two-photon photocurrents i_r, labeled ''classical'' in these figures. The calculations for the latter are based on the approach used by Bloch[9] and Teich.[11] However, to make as close a connection as possible between the entangled-photon [Eqs. (25)–(27)] and two-photon results, we determine the latter by numerically evaluating Eq. (A15) rather than by making use of Eq. (A16).

For all calculations, the pump wavelength is taken to be $\lambda_p=406$ nm ($\hbar\omega_p=3.054$ eV) and the down-converted photon-flux density is set at $\phi=5\times10^{19}$ photons/cm^2 sec. The minimum initial state energy $E_{i\,\min}$ that is able to conribute to the photoemission process is determined by requiring that $E_{i\,\min}+\hbar\omega_1+\hbar\omega_2$ be sufficient to overcome the work

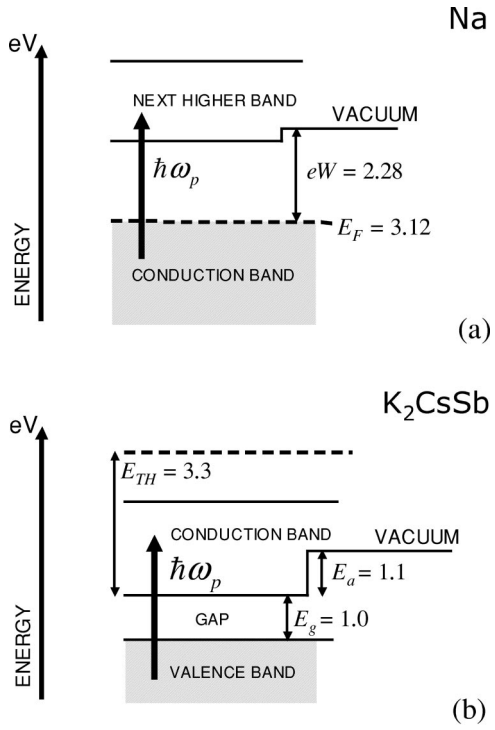

FIG. 1. (a) Two-photon absorption in sodium metal, with work function eW (eV) and Fermi energy E_F (eV). The energy of the photon pair is $E_p=\hbar\omega_p$. (b) Two-photon absorption in the bialkali semiconductor K_2CsSb, with electron affinity E_a (eV), band-gap energy E_g (eV), and electron-hole pair-production threshold E_{TH}.

function of the material. The escape depth d of the material, defined in the context of the usual three-step model for photoemission,[46,47] turns out to be approximately $d=400$ Å.[48] The calculations take the area of the illuminated spot to be $A=10^{-6}$ cm^2, corresponding to a spot size of 100 μm.

We now present the parameters that differ for sodium and bialkali semiconductor. The parameters used for Na metal

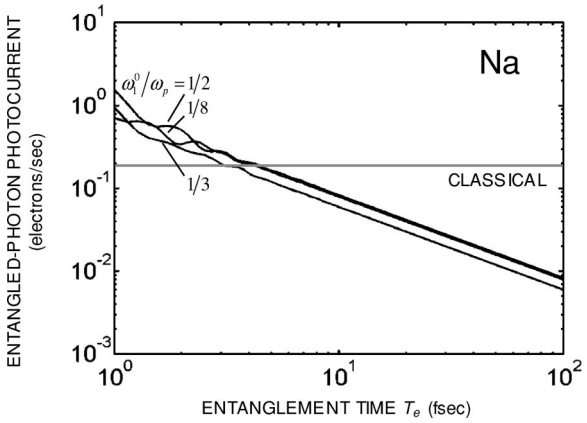

FIG. 2. Entangled-photon photocurrent calculated for a Na metal photocathode as a function of the entanglement time T_e, using nondegenerate photon pairs with nondegeneracy ratios $\omega_1^0/\omega_p=1-\omega_2^0/\omega_p=1/2$, 1/3, and 1/8. Parameter values for the calculations are $\tau_j=10$ fsec and $\phi=5\times10^{19}$ photons/cm^2 sec. The semiclassical two-photon photocurrent is shown for comparison.

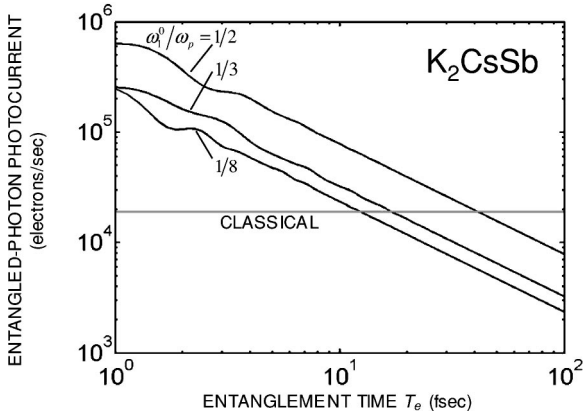

FIG. 3. Entangled-photon photocurrent calculated for a K_2CsSb bialkali photocathode as a function of the entanglement time T_e, using nondegenerate pairs with nondegeneracy ratios $\omega_1^0/\omega_p=1-\omega_2^0/\omega_p=1/2$, 1/3, and 1/8. Parameter values for the calculations are $\tau_j=270$ fsec and $\phi=5\times10^{19}$ photons/cm^2 sec. The semiclassical two-photon photocurrent is shown for comparison. The expected photocurrent is approximately five orders of magnitude greater than that for Na metal.

are (see Ref. 11, pp. 106–107) transmittance $\beta=0.05$, work function $eW=2.28$ eV, body-centered-cubic atomic density[42] $N=2.65\times10^{22}$ cm^{-3}, Fermi energy $E_F=3.12$ eV, Fermi wave number $k_F=0.9\times10^8$ cm^{-1}, intermediate-state lifetime $\tau_j=10$ fsec ($\kappa_j=10^{14}$), minimum intermediate-state energy $E_{j\,\min}=5.18$ eV, and maximum intermediate-state energy $E_{j\,\max}\approx8$ eV. The parameters used for K_2CsSb are[41,46,48,49] transmittance $\beta=0.7$ (obtained from the complex refractive index), work function $eW=2.1$ eV, primitive cell density $N=3.13\times10^{21}$ cm^{-3} for this body-centered-cubic structure,[48] electron affinity $E_A=1.1$ eV, band-gap energy $E_g=1.0$ eV, intermediate-state lifetime[50] $\tau_j=270$ fsec ($\kappa_j=3.7\times10^{12}$), minimum intermediate-state energy $E_{j\,\min}=2.5$ eV, and maximum intermediate-state energy $E_{j\,\max}=4.5$ eV.

The transition matrix element (transition "oscillator strength") for sodium metal is estimated to be[11] $[M]_{\mathrm{Na}}=8$, from which we obtain the average matrix element $\mu=8/N_j^2\approx1.7\times10^{-44}$ by use of Eq. (A13). The transition matrix element $[M]_{K_2CsSb}$ for K_2CsSb is estimated via Eq. (10c). Since the optical properties of bialkali antimonides, such as K_2CsSb, are similar to those of alkali antimonides such as K_3Sb and Cs_3Sb, the two-photon photocurrent yields cited by Teich[12] provide

$$\frac{\Lambda_{\mathrm{Na}}}{\Lambda_{K_2CsSb}}\approx10^{-5}. \tag{28}$$

Using Eq. (10c) leads to $[M]_{K_2CsSb}=4448$, which gives rise to an average matrix element $\mu=4448/N_j^2\approx2.7\times10^{-41}$.

Finally, in Figs. 4 and 5 we present the behavior of the photocurrent for different values of the intermediate-state lifetime τ_j, assuming energy-degenerate incident photons ($\omega10/\omega p=\frac{1}{2}$). The curves reveal that the entangled-photon photocurrent is essentially independent of the intermediate-state lifetime τ_j over a broad range.

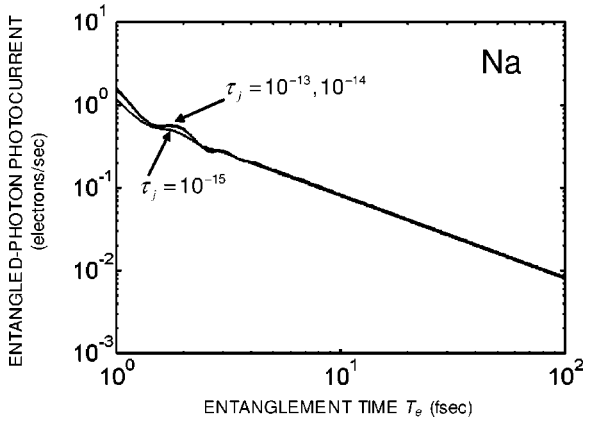

FIG. 4. Degenerate $(\omega_1^0/\omega_p = \omega_2^0/\omega_p = 1/2)$ entangled-photon photocurrent calculated for a sodium metal photocathode as a function of the entanglement time T_e assuming $\phi = 5\times 10^{19}$ and using different intermediate-state linewidths κ_j. The results scarcely depend on the lifetimes $\tau_j = 1/\kappa_j$.

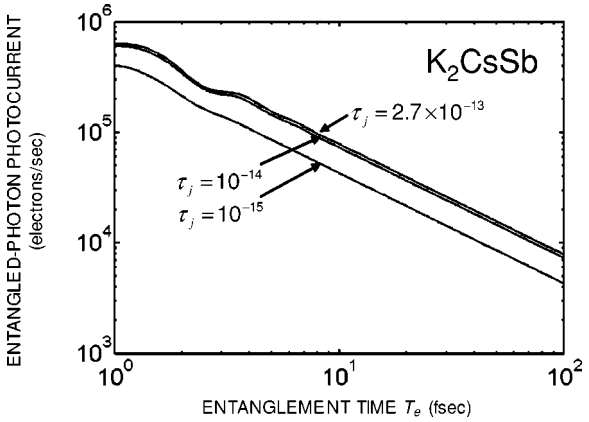

FIG. 5. Degenerate $(\omega_1^0/\omega_p = \omega_2^0/\omega_p = 1/2)$ entangled-photon photocurrent calculated for a bialkali photocathode as a function of the entanglement time T_e assuming $\phi = 5\times 10^{19}$ and using different intermediate-state linewidths κ_j. The results are only weakly dependent on the lifetimes $\tau_j = 1/\kappa_j$.

B. Entangled-photon quantum efficiency and cross section

Using the parameter values and entangled-photon photocurrent provided above, the entangled-photon quantum efficiency and cross section for Na metal are calculated via Eqs. (17) and (18) to be $\eta_e(\mathrm{Na}) = 1.6\times 10^{-15}$ and $\sigma_e(\mathrm{Na}) = 6.0 \times 10^{-30}$ cm^2, respectively, for $T_e = 10$ fsec. For K_2CsSb, these values are $\eta_e(K_2CsSb) = 1.6\times 10^{-9}$ and $\sigma_e(K_2CsSb) = 2.6\times 10^{-25}$ cm^2, respectively, also for $T_e = 10$ fsec. These cross sections are substantially smaller than those calculated for the $1S$-$2S$ transition in atomic hydrogen for an entangled-photon source with similar characteristics;[31] the disparity is likely a result of the fact that the latter interaction is resonant.

V. CONCLUSION

We have carried out calculations in second-order perturbation theory to estimate the photocurrent expected from Na metal and K_2CsSb semiconductor when entangled-photon pairs of entanglement time T_e elicit volume photoemission. The photocurrent varies inversely with entanglement time though subtle nonmonotonic behavior (resulting from interference) emerges over certain ranges of T_e. For sufficiently small values of T_e, the magnitude of the entangled photocurrent exceeds that of the semiclassical two-photon photocurrent. The results depend only weakly on the energy nondegeneracy of the entangled-photon pair and on the intermediate-state lifetime of the transition.

The entangled-photon photocurrent for K_2CsSb, which is calculated to be about five orders of magnitude greater than that for Na metal, should be readily observable inasmuch as the observation of far smaller two-photon photocurrents is commonplace. By virtue of their greater two-photon yield, even larger entangled-photon photocurrents would likely be obtained if organic photoemitters such as anthracene, tetracene, or perylene were used.[12]

ACKNOWLEDGMENTS

It is a pleasure to thank Professor Carlo G. Someda of the Università degli Studi di Padova, Italy, for valuable comments. A preliminary version of this work was presented to the Dipartimento di Elettronica e Informatica, Università degli Studi di Padova (Italy) for the Laurea (Dottore in Ingegneria) of F.L. in 1999. This work was supported by the U.S. National Science Foundation, the David & Lucile Packard Foundation, and the Center for Subsurface Imaging Systems (CenSSIS), an NSF Engineering Research Center.

APPENDIX

This appendix details the transformation of Eq. (24) into Eqs. (25)–(27).

Assuming that the transition matrix element varies slowly with j, ω_1, and ω_2, which is tantamount to considering an "average" matrix element throughout the band, and with the help of Eq. (22), the entangled-photon current in Eq. (24) can be written as

$$i_e = \phi\beta^2 e \frac{2Ad}{8\pi^3}(2\pi)^2 \frac{r_0^2 c^2}{\omega_1^0\omega_2^0}\frac{\pi}{4A_e T_e}\left[\left|\frac{\langle f|\hat{p}_x|j\rangle\langle j|\hat{p}_x|i\rangle}{m}\right|^2\right]_{\mathrm{av}} \frac{1}{N_j^2}\frac{(2m)^3}{4\pi^4\hbar^6}\sum_f \int\int\int \delta\left(\frac{E_f - E_i - \hbar\omega_p}{\hbar}\right)$$
$$\times\left|\int_{E_j\,\min}^{E_j\,\max}\left\{\frac{1-e^{-i(T_e/\hbar)(E_j-\hbar^2k^2/2m-\hbar\omega_1^0)-T_e\kappa_j/2}}{E_j-\hbar^2k^2/2m-\hbar\omega_1^0-i\hbar\kappa_j/2}+\frac{1-e^{-i(T_e/\hbar)(E_j-\hbar^2k^2/2m-\hbar\omega_2^0)-T_e\kappa_j/2}}{E_j-\hbar^2k^2/2m-\hbar\omega_2^0-i\hbar\kappa_j/2}\right\}\sqrt{E_j-E_c}\,dE_j\right|^2 dk_x dk_y dk_z. \quad \text{(A1)}$$

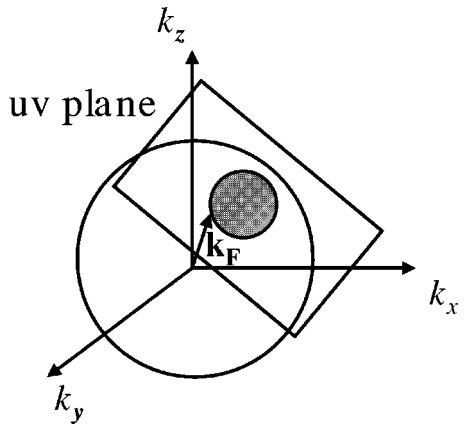

FIG. 6. Change of coordinate system in k space from (k_x,k_y,k_z) to (u,v,w) and intersection of the u-v plane with the Fermi surface of the material, where $\mathbf{k}_\mathrm{F}$ corresponds to the Fermi energy E_F.

We proceed to take a number of steps to simplify the triple integral in Eq. (A1) to a single integral, which we ultimately evaluate numerically.

To begin, as illustrated in Fig. 6, a change of coordinates[9] from k_x,k_y,k_z to u,v,w is effected,

$$dk_x dk_y dk_z \rightarrow du\,dv\,dw, \tag{A2}$$

such that (u, v) is a plane of constant energy difference and w is normal to that plane. This is consistent with the conservation of the crystal momentum. To carry out the integration over dw, it is convenient to make use of a Maclaurin expansion of $\varepsilon = E_f - E_i - \hbar\omega_p$,[9,10] so that

$$\varepsilon = \varepsilon_0 + \left.\frac{\partial\varepsilon}{\partial w}\right|_{w=0} w, \tag{A3}$$

where $\varepsilon_0 = 0$ and

$$\varepsilon = \frac{\hbar^2}{2m}[(k+g)^2 - k^2] - \hbar\omega_p = \frac{\hbar^2}{2m}(2kg+g^2) - \hbar\omega_p. \tag{A4}$$

Thus $(\partial\varepsilon/\partial w)|_{w=0} = (\partial\varepsilon/\partial k)|_{k=c} = (\hbar^2/m)\,g$, where g is the gain in momentum associated with the absorption of the two photons and c is a constant.

Using the properties of the δ function then yields

$$\begin{aligned}
&\int_{-\infty}^{+\infty} \delta\left(\frac{E_f - E_i - \hbar\omega_p}{\hbar}\right) F(k,T_e)\; dw \\
&= \int_{-\infty}^{+\infty} \delta\left(w \frac{1}{\hbar}\left.\frac{\partial\varepsilon}{\partial w}\right|_{w=0}\right) F(k,T_e)\; dw \\
&= \frac{m}{\hbar}\frac{1}{g}\int_{-\infty}^{+\infty} \delta(w) F(k,T_e)\; dw \\
&= \frac{m}{\hbar}\frac{1}{g} F(k|_{\mathrm{circle}},T_e),
\end{aligned} \tag{A5}$$

where F is explicitly written as

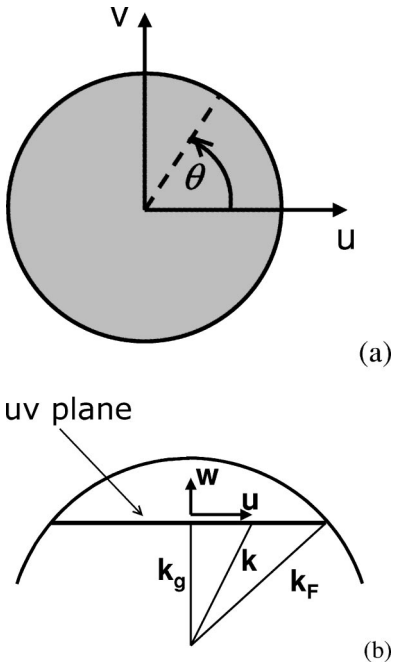

FIG. 7. Change of coordinates (a) from $du\,dv$ to $u\,du\,d\theta$ and (b) thence to $k\,dk$.

$$\begin{aligned}
F(k,T_e) = \Bigg| \int_{E_{j\,\min}}^{E_{j\,\max}} \Bigg\{ &\frac{1 - e^{-i(T_e/\hbar)(E_j - \hbar^2k^2/2m - \hbar\omega_1^0) - T_e\kappa_j/2}}{E_j - \hbar^2k^2/2m - \hbar\omega_1^0 - i\hbar\kappa_j/2} \\
&+ \frac{1 - e^{-i(T_e/\hbar)(E_j - \hbar^2k^2/2m - \hbar\omega_2^0) - T_e\kappa_j/2}}{E_j - \hbar^2k^2/2m - \hbar\omega_2^0 - i\hbar\kappa_j/2} \Bigg\} \\
&\times \sqrt{E_j - E_c}\; dE_j \Bigg|^2
\end{aligned} \tag{A6}$$

with $k = \sqrt{2mE_i/\hbar^2}$.

The surface under consideration is determined by the intersection of the uv plane and the surface of constant energy specified by the condition $k = k_{\max}$; the former is a circle if the latter is a sphere. This is a good approximation for sodium, where $k = k_{\max} = k_F$ represents the Fermi surface, and it suffices for K_2CsSb as well. The triple integral is then reduced to a double integral over the circle on the uv plane:

$$\begin{aligned}
&\sum_f \int\int\int \delta\left(\frac{E_f - E_i - \hbar\omega_p}{\hbar}\right) F(E_i,T_e)\; dk_x dk_y dk_z \\
&\quad = \frac{m}{\hbar}\sum_f \frac{1}{g_f}\int_{\mathrm{circle}}\int F(k|_{\mathrm{circle}},T_e)\; du dv.
\end{aligned} \tag{A7}$$

Transforming to polar coordinates with $du\,dv = u\,du\,d\theta$, as illustrated in Fig. 7(a), we integrate over $d\theta$ on the circle, yielding 2π. With a further change of variable from u to k via $u = \sqrt{k^2 - k_g^2}$, so that $du = dk\; k/\sqrt{k^2 - k_g^2}$, as evidenced in Fig. 7(b), we arrive at a single integral over dk and Eq. (A7) simplifies to

$$\frac{m}{\hbar}\sum_f \frac{1}{g_f} 2\pi \int F(k,T_e)\, u\, du = \frac{m}{\hbar}\sum_f \frac{1}{g_f} 2\pi \int_{k_{\min}}^{k_F} F(k,T_e)\, k\, dk, \tag{A8}$$

where $k_F = \sqrt{2mE_F/\hbar^2}$ is associated with the Fermi energy. The lower limit of the integral, $k_{\min}$, is determined by imposing the condition that the gain in electron energy is adequate to overcome the work function of the material W,

$$k \geqslant \sqrt{k_F^2 + k_W^2 - \frac{2m}{\hbar^2}\hbar\omega_p} = k_F\sqrt{1 + \frac{W}{E_F} - \frac{\hbar\omega_p}{E_F}} = k_{\min}, \tag{A9}$$

with $k_W = \sqrt{2mW/\hbar^2}$.

The contraction from the double integral in Eq. (A7) to the single integral in Eq. (A8) thus results from the following sequence of transformations:

$$\sum_f \frac{1}{g_f}\int\int_{\text{circle}} F(k|_{\text{circle}}, T_e)\, du dv \rightarrow \int\int_{\text{circle}} \frac{F(k|_{\text{circle}}, T_e)}{g}\, du dv = 2\pi \int_{k_{\min}}^{k_F} \frac{F(k,T_e)}{\sqrt{k^2 + (2m/\hbar^2)\hbar\omega_p} - k}\, k\, dk, \tag{A10}$$

where g is determined by the condition

$$k + g = \sqrt{k^2 + \frac{2m}{\hbar^2}\hbar\omega_p}, \tag{A11}$$

which simply states that $\hbar\omega_p$ is the energy gained by the absorption of the two photons.

Comparing Eq. (A10) for entangled-photon photoemission with Eq. (A15) for two-photon photoemission reveals that the distinction lies in the presence of the quantity $F(k,T_e)$ in the former. This integral, set forth in Eq. (A6), contains the interference terms that are characteristic of entangled photons, as well as the density of states included in the present treatment.

Combining the foregoing results, the entangled-photon photocurrent in Eq. (A1) simplifies to

$$i_e = \phi\beta^2 e \frac{2Ad}{8\pi^3}(2\pi)^2 \frac{r_0^2 c^2}{\omega_1^0 \omega_2^0}\frac{\pi}{4A_e T_e}\left[\left|\frac{\langle f|\hat{p}_x|j\rangle\langle j|\hat{p}_x|i\rangle}{m}\right|^2\right]_{av} \times \frac{1}{N_j^2}\frac{(2m)^3}{4\pi^4\hbar^6}\frac{m}{\hbar} 2\pi \int_{k_{\min}}^{k_F} \frac{F(k,T_e)}{\sqrt{k^2 + (2m/\hbar^2)\hbar\omega_p} - k}\, k\, dk \tag{A12}$$

where $F(k,T_e)$ is defined in Eq. (A6). Reordering the terms and making use of Eqs. (23) and (27), viz.,

$$\mu = \left[\left|\frac{4\langle f|\hat{p}_x|j\rangle\langle j|\hat{p}_x|i\rangle}{m\hbar\omega_p}\right|^2\right]_{\text{av}} \Big/ N_j^2,$$

$$N_j = \int_{E_{j\,\min}=E_c}^{E_{j\,\max}} \rho(E_j)\, dE_j, \tag{A13}$$

finally leads to

$$i_e = \phi\beta^2 A d \frac{e m^4 r_0^2 c^2}{4\pi^3\hbar^5}\frac{\omega_p^2}{4\omega_1^0\omega_2^0}\mu\frac{1}{A_e T_e} \times \int_{k_{\min}}^{k_F} \frac{F(k,T_e)}{\sqrt{k^2 + (2m/\hbar^2)\hbar\omega_p} - k}\, k\, dk, \tag{A14}$$

which is identical to Eq. (25) as promised. The average matrix element μ in Eq. (A13) is appropriate for transitions through a band of intermediate states to a band of final states, where N_j is the number density of intermediate states. The matrix element M in Eq. (7), in contrast, is appropriate for a small number of discrete intermediate states.

Since the double integral in Eq. (A14) does not have a closed-form solution, it is evaluated numerically via direct calculation using MATLAB.

Inasmuch as Eq. (16) of Ref. 9 for two-photon photoemission, which is analogous to Eq. (A10) for entangled-photon photoemission, is called upon throughout, it is reproduced here for convenience:

$$\sum_f \frac{1}{g_f}\int\int_{\text{circle}} du dv \rightarrow \int\int_{\text{circle}} \frac{du dv}{g} = 2\pi \int_{k_{\min}}^{k_F} \frac{k\, dk}{\sqrt{k^2 + (2m/\hbar^2)2\hbar\omega} - k}. \tag{A15}$$

In this case, the single integral in dk simplifies to a closed form expression under the approximation $\hbar^2 k^2/2m > 2\hbar\omega$, which yields Eq. (17a) of Ref. 9, which is again reproduced for convenience:

$$\int\int_{\text{circle}} \frac{du dv}{g} = \frac{4}{3}\,\pi\,\frac{E_F}{2\hbar\omega}\,k_F\left[1 + \frac{eW}{E_F} - \frac{2\hbar\omega}{E_F}\right]^{3/2}. \tag{A16}$$

*Email address: cescol@libero.it
†Email address: teich@bu.edu
‡URL: http://www.bu.edu/qil

[1] N. Bloembergen, *Nonlinear Optics* (W. A. Benjamin, Reading, MA, 1977).
[2] M. C. Teich, J. M. Schroeer, and G. J. Wolga, Phys. Rev. Lett. **13**, 611 (1964).
[3] H. Sonnenberg, H. Heffner, and W. Spicer, Appl. Phys. Lett. **5**, 95 (1964).
[4] S. Schuppler, N. Fischer, T. Fauster, and W. Steinmann, Phys. Rev. B **46**, 13 539 (1992).
[5] X. Y. Wang, R. Paiella, and R. M. Osgood, Jr., Phys. Rev. B **51**, 17 035 (1995).
[6] T. Fauster, Surf. Sci. **507**, 256 (2002).
[7] L. Toben, T. Hannappel, R. Eichberger, K. Moller, L. Gundlach, R. Ernstorfer, and F. Willig, J. Cryst. Growth **248**, 206 (2003).
[8] R. L. Smith, Phys. Rev. **128**, 2225 (1962).
[9] P. Bloch, J. Appl. Phys. **35**, 2052 (1964).
[10] H. Y. Fan, Phys. Rev. **68**, 43 (1945).
[11] M. C. Teich, Ph.D. thesis, Cornell University, 1966 (*Two Quantum Photoemission and dc Photomixing in Sodium*, Pro Quest Information and Learning, http://wwwlib.umi.com/dxweb/gateway, No. 6606082).
[12] M. C. Teich and G. J. Wolga, Phys. Rev. **171**, 809 (1968).
[13] M. C. Teich and G. J. Wolga, Phys. Rev. Lett. **16**, 625 (1966).
[14] M. C. Teich and B. E. A. Saleh, Quantum Opt. **1**, 153 (1989).
[15] D. N. Klyshko, *Photons and Nonlinear Optics* (Nauka, Moscow, 1980, Gordon and Breach, New York, 1988), Chaps. 1 and 6.
[16] L. Mandel and E. Wolf, *Optical Coherence and Quantum Optics* (Cambridge University Press, New York, 1995).
[17] J. Peřina, Z. Hradil, and B. Jurčo, *Quantum Optics and Fundamentals of Physics* (Kluwer, Boston, 1994).
[18] D. N. Klyshko, Pis'ma Zh. Eksp. Teor. Fiz. **6**, 490 (1967) [JETP Lett. **6**, 23 (1967)].
[19] T. G. Giallorenzi and C. L. Tang, Phys. Rev. **166**, 225 (1968).
[20] S. E. Harris, M. K. Oshman, and R. L. Byer, Phys. Rev. Lett. **18**, 732 (1967).
[21] D. Magde and H. Mahr, Phys. Rev. Lett. **18**, 905 (1967).
[22] M. Atatüre, G. Di Giuseppe, M. D. Shaw, A. V. Sergienko, B. E. A. Saleh, and M. C. Teich, Phys. Rev. A **66**, 023822 (2002).
[23] A. Joobeur, B. E. A. Saleh, T. S. Larchuk, and M. C. Teich, Phys. Rev. A **53**, 4360 (1996).
[24] B. E. A. Saleh, A. F. Abouraddy, A. V. Sergienko, and M. C. Teich, Phys. Rev. A **62**, 043816 (2000).
[25] A. F. Abouraddy, B. E. A. Saleh, A. V. Sergienko, and M. C. Teich, J. Opt. Soc. Am. B **19**, 1174 (2002).
[26] M. B. Nasr, A. F. Abouraddy, M. C. Booth, B. E. A. Saleh, A. V. Sergienko, M. C. Teich, M. Kempe, and R. Wolleschensky, Phys. Rev. A **65**, 023816 (2002).
[27] D. C. Burnham and D. L. Weinberg, Phys. Rev. Lett. **25**, 84 (1970).
[28] T. S. Larchuk, M. C. Teich, and B. E. A. Saleh, Ann. N.Y. Acad. Sci. **755**, 680 (1995).
[29] S. Friberg, C. K. Hong, and L. Mandel, Opt. Commun. **54**, 311 (1985).
[30] J. Javanainen and P. L. Gould, Phys. Rev. A **41**, 5088 (1990).
[31] H.-B. Fei, B. M. Jost, S. Popescu, B. E. A. Saleh, and M. C. Teich, Phys. Rev. Lett. **78**, 1679 (1997).
[32] J. Peřina, Jr., B. E. A. Saleh, and M. C. Teich, Phys. Rev. A **57**, 3972 (1998).
[33] B. E. A. Saleh, B. M. Jost, H.-B. Fei, and M. C. Teich, Phys. Rev. Lett. **80**, 3483 (1998).
[34] M. C. Teich and B. E. A. Saleh, Cesk. Cas. Fyz. **47**, 3 (1997).
[35] A. N. Boto, P. Kok, D. S. Abrams, S. L. Braunstein, C. P. Williams, and J. P. Dowling, Phys. Rev. Lett. **85**, 2733 (2000).
[36] A. H. Sommer, Appl. Phys. Lett. **3**, 62 (1963).
[37] M. Göppert-Mayer, Ann. Phys. (Leipzig) **9**, 273 (1931).
[38] H. B. Bebb and A. Gold, Phys. Rev. **143**, 1 (1966).
[39] P. Lambropoulos, Phys. Rev. A **9**, 1992 (1974).
[40] L. I. Schiff, *Quantum Mechanics* (McGraw-Hill, New York, 1955).
[41] C. Ghosh, Phys. Rev. B **22**, 1972 (1980).
[42] C. Kittel, *Introduction to Solid Sate Physics*, 7th ed. (Wiley, New York, 1996).
[43] M. C. Teich and G. J. Wolga, J. Opt. Soc. Am. **57**, 542 (1967).
[44] W. E. Spicer, Phys. Rev. **112**, 114 (1958).
[45] B. E. A. Saleh and M. C. Teich, *Fundamentals of Photonics* (Wiley, New York, 1991).
[46] A. H. Sommer, *Photoemissive Materials* (Wiley, New York, 1968).
[47] C. Ghosh, Proc. SPIE **346**, 62 (1982).
[48] C. Ghosh, in *Physics of Thin Films, Advances in Research and Development*, Vol. 12, edited by G. Hass, M. H. Francombe, and J. L. Vossen (Academic, New York, 1982).
[49] R. Nathan and C. H. B. Mee, Phys. Status Solidi A **2**, 67 (1970).
[50] H. Hattori, Y. Kawashima, M. Daikoku, H. Inouye, and H. Nakatsuka, Jpn. J. Appl. Phys., Part 1 **39**, 4793 (2000).